J|A|C|S
ARTICLES
Published on Web 09/10/2002

Dynamic Simulations of Adhesion and Friction in Chemical Force Microscopy

Yongsheng Leng† and Shaoyi Jiang*

Contribution from the Department of Chemical Engineering, University of Washington, Box 351750, Seattle, Washington 98195-1750

Received March 21, 2002

Abstract: A hybrid molecular simulation approach has been applied to investigate dynamic adhesion and friction between a chemical force microscope (CFM) tip and a substrate, both modified by self-assembled monolayers (SAMs) with hydrophobic methyl (CH_3) or hydrophilic hydroxyl (OH) terminal groups. The method combines a dynamic model for the CFM tip−cantilever system and a molecular dynamics (MD) relaxation technique for SAMs on Au(111) at room temperature. The hybrid simulation method allows one to simulate force−distance curves (or adhesion) and friction loops (or friction coefficient) in the CFM on the experimental time scale for the first time. The simulation results also provide valuable molecular information at the interface that is not accessible in CFM experiments, such as the actual tip position with respect to the cantilever support position, molecular and hydrogen-bonding structures at the interface, and load distributions among different molecular chains (or single-molecule forces). Results show that the adhesion force and friction coefficient for the OH/OH contact pair are much larger than those for the CH_3/CH_3 pair due to the formation of hydrogen bonds. During the retraction of a CFM tip from a surface, the CFM tip is away from the sample surface slightly while the spring undergoes dramatic elongation in the normal direction before rupture occurs. Single-molecule forces are distributed unevenly at the contact area. Surface energies calculated for functionalized surfaces compare well with those determined by experiments.

Introduction

Chemical force microscopy (CFM)[1] provides a method for probing molecular interactions and imaging surfaces with chemical sensitivity. By covalently modifying atomic force microscope (AFM) tips and substrates with self-assembled monolayers (SAMs) that terminate in distinct functional groups, one is able to apply this technique to measure adhesion and friction forces between various probe tips and substrates with specific surface chemistry.[1−5] A similar approach was applied to study single-bond forces[6−8] upon rupture and molecular interactions in biological systems.[9] In parallel, molecular dynamics (MD) simulations have been performed to investigate the indentation and friction properties of SAMs[10−12] and the rupture of adhesive films bonded to solid substrates.[13] However, the difference in the time scale between conventional MD simulations and AFM or CFM experiments is 6 orders of magnitude or more. Contact mechanics and detailed molecular information near the contact area in CFM are not fully understood yet. Due to the complexity of the system involved, no study has been performed to simulate force curves and friction loops in CFM on the experimental time scale so far.

In this work, we applied a temporally hybrid molecular simulation method that we developed recently[14,15] to simulate adhesion and friction between SAM-modified AFM tips and surfaces on the experimental time scale. For simple organic systems, such as alkanethiol monolayers on Au (111), the characteristic vibration frequency of the films is much greater than the resonant frequency of a CFM cantilever. Therefore, the energy modes between them can be decoupled.[15] Since the relaxation of SAMs upon perturbation due to the movement of a CFM tip is quite fast, the dynamic equations of the CFM tip can be integrated separately from the MD relaxation of SAMs. This hybrid approach maintains the continuity of tip motion

* Corresponding author. E-mail: sjiang@u.washington.edu.
† Present address: Department of Chemical Engineering, Vanderbilt University, Nashville, TN 37235-1604, and Chemical Sciences Division, Oak Ridge National Laboratory, Oak Ridge, TN 37831-6110. E-mail: yongsheng.leng@vanderbilt.edu.

(1) (a) Noy, A.; Frisbie, C. D.; Rozsnyai, L. F.; Wrighton, M. S.; Lieber, C. M. *J. Am. Chem. Soc.* **1995**, *117*, 7943. (b) Noy, A.; Vezenov, D. V.; Lieber, C. M. *Annu. Rev. Mater. Sci.* **1997**, *27*, 381.
(2) Thomas, R. C.; Houston, J. E.; Crooks, R. M.; Kim, T.; Michalske, T. A. *J. Am. Chem. Soc.* **1995**, *117*, 3830.
(3) Green, J.-B. D.; McDermott, M. T.; Porter, M. D.; Siperko, L. M. *J. Phys. Chem.* **1995**, *99*, 10960.
(4) van der Vegte, E. W.; Hadziioannou, G. *Langmuir* **1997**, *13*, 4357.
(5) Sinniah, S. K.; Steel, A. B.; Miller, C. J.; Reutt-Robey, J. E. *J. Am. Chem. Soc.* **1996**, *118*, 8925.
(6) Williams, J. M.; Han, T. J.; Beebe, T. P., Jr. *Langmuir* **1996**, *12*, 1291.
(7) Wei, Z. Q.; Wang, C.; Zhu, C. F.; Zhou, C. Q.; Xu, B.; Bai, C. L. *Surf. Sci.* **2000**, *459*, 401.
(8) (a) Skulason, H.; Frisbie, C. D. *J. Am. Chem. Soc.* **2000**, *122*, 9750. (b) Skulason, H.; Frisbie, C. D. *Langmuir* **2000**, *16*, 6294.
(9) (a) Florin, E.-L.; Moy, V. T.; Gaub, H. E. *Science* **1994**, *264*, 415. (b) Grandbois, M.; Beyer, M.; Rief, M.; Clausen-Schaumann, H.; Gaub, H. E. *Science* **1999**, *283*, 1727.
(10) Glosli, J. N.; McClelland, G. M. *Phys. Rev. Lett.* **1993**, *70*, 1960.
(11) (a) Tupper, K. J.; Colton, R. J.; Brenner, D. W. *Langmuir* **1994**, *10*, 2041. (b) Tupper, K. J.; Brenner, D. W. *Thin Solid Films* **1994**, *253*, 185.
(12) (a) Mikulski, P. T.; Harrison, J. A. *J. Am. Chem. Soc.* **2001**, *123*, 6873. (b) Mikulski, P. T.; Harrison, J. A. *Tribol. Lett.* **2001**, *10*, 29.
(13) Baljon, A. R. C.; Robbins, M. O. *Science* **1996**, *271*, 482.
(14) Leng, Y. S.; Jiang, S. *J. Chem. Phys.* **2000**, *113*, 8800.
(15) Leng, Y. S.; Jiang, S. *Phys. Rev. B* **2001**, *63*, 193406.

10.1021/ja026274z CCC: $22.00

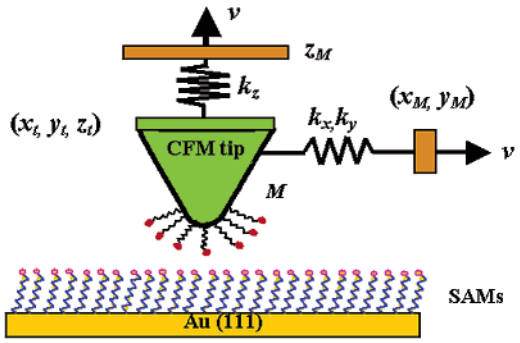

Figure 1. Mechanical model for the simulation system.

with the discrete jump of molecular configurations of SAMs. In this work, we focus on two contact pairs, hydrophobic methyl/methyl (CH_3/CH_3)-terminated SAMs and hydrophilic hydroxyl/hydroxyl (OH/OH)-terminated SAMs. While molecular interactions are due to van der Waals interactions for the CH_3/CH_3 pair, hydrogen bonding plays a very important role for the OH/OH pair. Simulation results reveal many interesting microscopic processes underlying CFM experiments.

Potential Models and Simulation Methodology

CFM Tips and Substrates. The model tip is a gold cluster composed of 351 Au atoms with four (111) planes and two (001) planes. The gold cluster was optimized using the many-body Glue model potential.[16] Alkanethiol chains, $[-S(CH_2)_7CH_3]_{40}$ or $[-S(CH_2)_7OH]_{40}$, were then attached onto the four surrounding (111) and the bottom (001) facets. The arrangement of sulfur atoms on the Au facets was as reported by Luedtke and Landman.[17] These chains were then allowed to evolve at 300 K through MD relaxation. For the interactions of SAM chains, the united-atom (UA) model[18,19] was used, including intrachain bond bending and torsional interactions and nonbonded Lennard-Jones (LJ) 12-6 interactions between atoms in different chains and within the same chain, but separated by more than three UA atoms ($\sigma_{CH_3-CH_3} = 3.905$ Å, $\epsilon_{CH_3-CH_3} = 88.1$ K; $\sigma_{CH_2-CH_2} = 3.905$ Å, $\epsilon_{CH_2-CH_2} = 59.4$ K; $\sigma_{S-S} = 3.55$ Å, $\epsilon_{S-S} = 126$ K; $\sigma_{O-O} = 3.07$ Å, $\epsilon_{O-O} = 85.6$ K; and $\sigma_{H-H} = 0.0$ Å, $\epsilon_{H-H} = 0.0$ K). Bond lengths for CH_x-CH_x ($x = 2$ or 3), S−CH_2, CH_2−O, and O−H were held constant via the RATTLE algorithm[20] at 1.53, 1.82, 1.43, and 0.945 Å,[18,19] respectively. For interactions between SAMs and the Au substrate, the Morse potential for Au−S ($D_e = 4235.7$ K, $r_e = 2.7$ Å, $\alpha = 1.47$ Å^{-1}) and the LJ 12-6 potential for Au−UA atom ($\sigma_{Au-CH_3} = 3.632$ Å, $\epsilon_{Au-CH_3} = 71.9$ K; $\sigma_{Au-CH_2} = 3.632$ Å, $\epsilon_{Au-CH_2} = 52$ K),[21] Au−O ($\sigma_{Au-O} = 3.22$ Å, $\epsilon_{Au-O} = 62.4$ K), and Au−H ($\sigma_{Au-H} = 0.0$ Å, $\epsilon_{Au-H} = 0.0$ K)[22] were used. At 300 K, SAMs remain the $\sqrt{3}\times\sqrt{3}$R30° packing structure. For the gold substrate, the Glue model potential[16] was used. For OH-terminated SAMs, the interaction parameters, including partial charges, bond angles, and torsions, were taken from the optimized potential for liquid simulation (OPLS) model.[19,23]

The substrate was composed of seven Au (111) layers, with each layer consisting of 600 Au atoms. Two hundred SAM chains were placed on Au (111) substrates.[24−27] The Au atoms in the bottom layer were held rigid. The remaining six layers of Au atoms were allowed to move via the Brownian dynamics algorithm[28] with the temperature

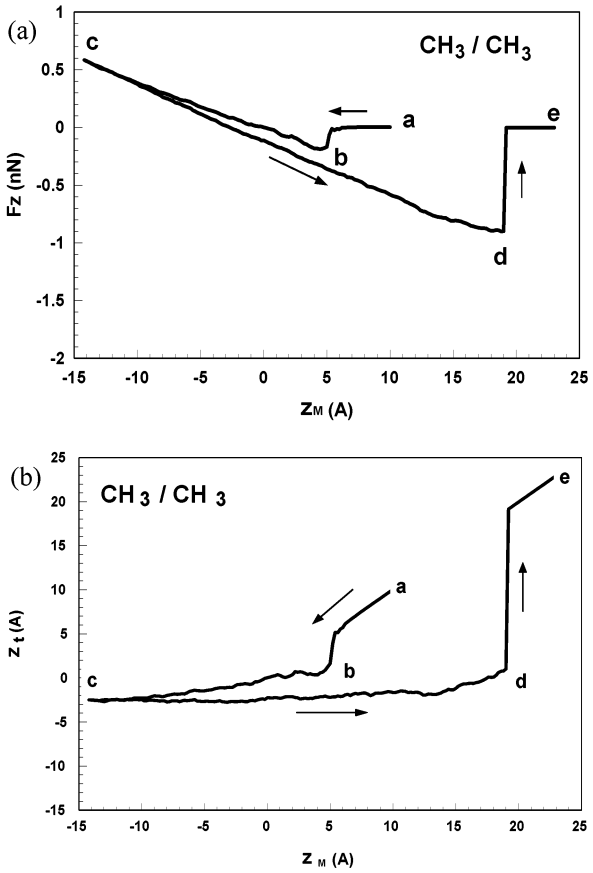

Figure 2. Force−distance curve (a) and tip position z_t versus support position z_M (b) for the CH_3/CH_3 contact pair.

controlled at 300 K. On the top layer, Au−Au distances around adsorption sites of S were elongated. At low temperature, we found this elongation was about 14∼21%, which is consistent with the results of ab initio calculations reported by Gronbeck et al.[27] for the adsorption of SCH_3 thiolates on a Au (111) surface.

Hybrid Simulation Method. Figure 1 shows the mechanical model of our simulation system. In simulations of adhesion, the CFM tip was dragged by the support (z_M) through the spring (k_z) at a velocity v while the support (x_M,y_M) was fixed. In simulations of lateral friction, the CFM tip was dragged by the support (x_M,y_M) with constant y_M through the spring (k_x) at a velocity v while the support (z_M) was fixed for constant-height scanning.[29] The equations of motion for the CFM tip are given by

$$M\ddot{x}_t = k_x(x_M - x_t) + W_x(x_t,y_t,z_t;X(t)) \quad (1)$$

$$M\ddot{y}_t = k_y(y_M - y_t) + W_y(x_t,y_t,z_t;X(t)) \quad (2)$$

$$M\ddot{z}_t = k_z(z_M - z_t) + W_z(x_t,y_t,z_t;X(t)) \quad (3)$$

(16) Ercolessi, F.; Parrinello, M.; Tosatti, E. *Philos. Mag. A* **1988**, *58*, 213.
(17) Luedtke, W. D.; Landman, U. *J. Phys. Chem. B* **1998**, *102*, 6566.
(18) Hautman, J.; Klein, M. L. *J. Chem. Phys.* **1989**, *91*, 4994.
(19) Hautman, J.; Bareman, J. P.; Mar, W.; Klein, M. L. *J. Chem. Soc., Faraday Trans.* **1991**, *87*, 2031.
(20) Andersen, H. C. *J. Comput. Phys.* **1983**, *52*, 24.
(21) Mahaffy, R.; Bhatia, R.; Garrison, B. J. *J. Phys. Chem. B* **1997**, *101*, 771.
(22) LJ parameters for Au−O and Au−H were calculated from those of CH_2−CH_2, Au−CH_2,[19] O−O, and H−H[18] using the geometric mean method.
(23) Jorgensen, W. L. *J. Phys. Chem.* **1986**, *90*, 1276.
(24) Parameters in the Morse potential[21] were obtained on the basis of ab initio calculations for the adsorption of SCH_3 on the hcp hollow site of Au (111) by Sellers et al.[25] Recent quantum chemical calculations[26,27] show that the fcc 3-fold hollow site is energetically favorable over the hcp site by 1 kcal/mol. However, this difference should not have much effect on the calculated CFM force−distance curves.
(25) Sellers, H.; Ulman, A.; Shnidman, Y.; Eilers, J. E. *J. Am. Chem. Soc.* **1993**, *115*, 9389.
(26) Beardmore, K. M.; Kress, J. D.; Gronbech-Jensen, N.; Bishop, A. R. *Chem. Phys. Lett.* **1998**, *286*, 40.
(27) Gronbeck, H.; Curioni, A.; Andreoni, W. *J. Am. Chem. Soc.* **2000**, *122*, 3839.
(28) van Gunsteren, W. F.; Berendsen, H. J. C. *Mol. Phys.* **1982**, *45*, 637.
(29) For constant-force scanning, eq 3 is given in ref 14.

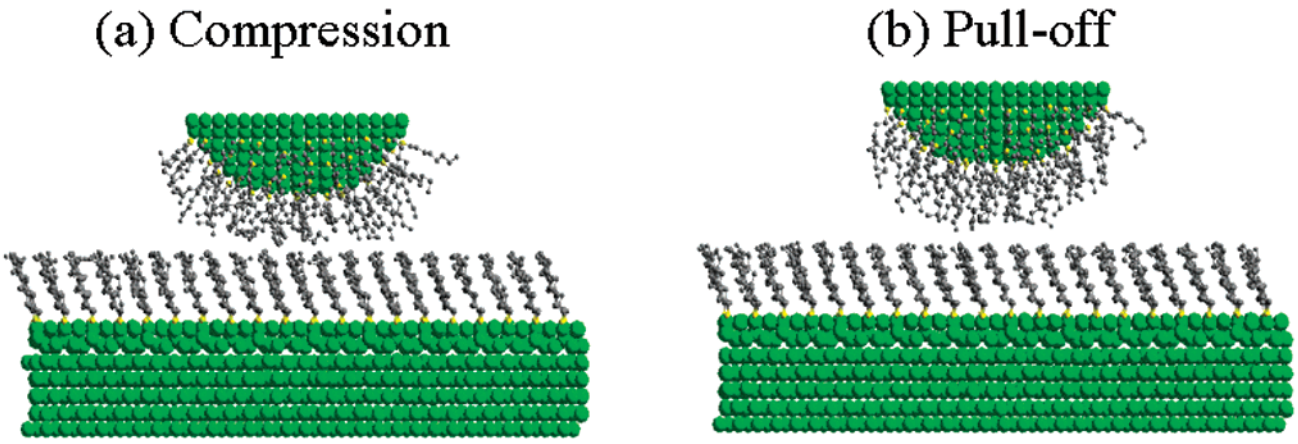

Figure 3. Molecular configurations for the CH_3/CH_3 contact pair at (a) compression (stage c) and (b) pull-off (stage d).

For adhesion simulations,

$$z_M = vt, \quad x_M = y_M = \text{const.} \tag{4}$$

The measured normal force is given by

$$F_z = k_z(z_M - z_t) \tag{5}$$

For friction simulations,

$$x_M = vt, \quad y_M = z_M = \text{const.} \tag{6}$$

The measured friction force is given by

$$F_x = k_x(x_M - x_t) \tag{7}$$

In the equations above, the coordinates (x_t,y_t,z_t) denote the instantaneous position of the CFM tip at time t, and M is the effective mass of the tip−cantilever system. The surface interaction forces W_x, W_y, and W_z depend not only on the tip position (x_t,y_t,z_t) but also on the molecular configuration $X(t)$ of the SAM film and the substrate at time t. The mechanical parameters used in our simulations are given as follows: effective mass of the CFM tip, $M = 10^{-11}$ kg; approaching/retracting or scanning velocity, $v = 400$ nm/s; and spring constants, $k_x = 132$ N/m, $k_y = 100$ N/m, and $k_z = 0.5$ N/m.[30] We integrate the equations of motion for the tip over $100\Delta t_{tip}$, where the time step $\Delta t_{tip} = 0.25\ \mu$s (equivalent to displacement of the support by 0.01 nm) using a backward differation (BD) algorithm. We then relax the SAM film and Au substrate over $300\Delta t_{MD}$, with a MD time step $\Delta t_{MD} = 3$ fs. MD relaxation over 300, 600, and $1200\Delta t_{MD}$ yields the same force−distance curve, indicating that the relaxation of SAMs and Au substrate is quite fast.

Results and Discussion

Force−Distance Curves and Adhesion. Many measurements of force−distance curves in CFM experiments were performed in liquid to reduce capillary forces that mask tip−sample interactions.[1,4−7] The effect of solvent on the adhesion mechanics of contact pairs is quite complicated.[5] The molecular simulation method is well suited to study these interactions and reveal detailed molecular structures at the interface. In this work, we concentrate on two interfaces in a vacuum created by CH_3/CH_3 (hydrophobic) and OH/OH (hydrophilic) pairs. Figure 2a shows the force−distance curve for an approach−retraction process for the CH_3/CH_3 contact pair. The CFM tip experiences typical jump-to-contact (b), compression (c), and pull-off (d) stages. It can be seen from Figure 2a that, at the pull-off stage, the molecular adhesion force (F_{adh}) reaches −0.9 nN. From the Johnson−Kendall−Roberts (JKR) theory of adhesion mechanics,[31] adhesion force is given by

$$F_{adh} = -\frac{3}{2}\pi RW \tag{8}$$

For the CH_3/CH_3 contact pair, the reversible adhesion work $W = 2\gamma_{CH_3}$, where γ_{CH_3} is the surface energy per unit area for CH_3-terminated SAMs. The tip radius is estimated as $R = 3$ nm. The surface energy γ_{CH_3} is calculated to be 32 mJ/m^2. This value

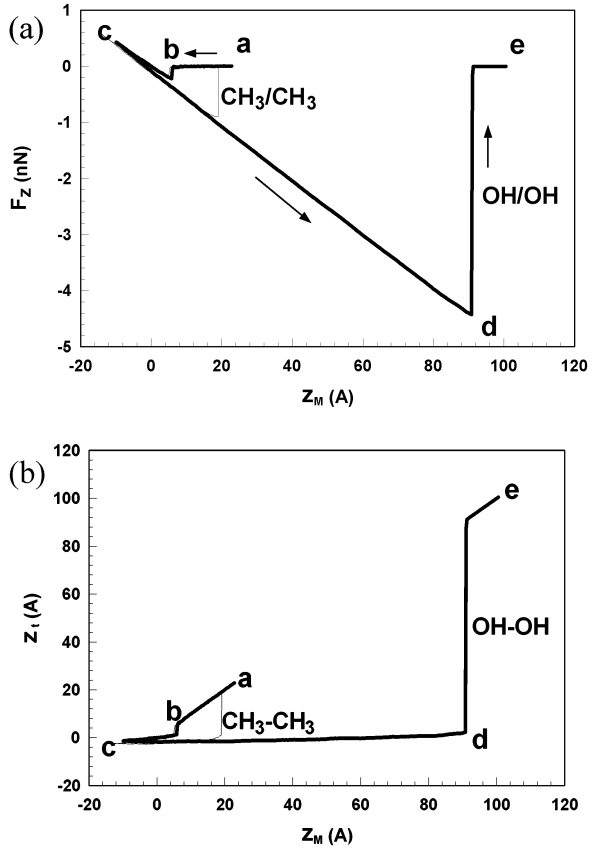

Figure 4. Force−distance curve (a) and tip position z_t versus support position z_M (b) for the OH/OH contact pair. Comparison with the CH_3/CH_3 pair is also shown.

(30) Many CFM experiments were done using a spring constant k_z that was 1 order of magnitude smaller, e.g., 0.04−0.06 N/m. This would generate a larger elongation of the cantilever, i.e., larger z_M in Figures 2 and 4.

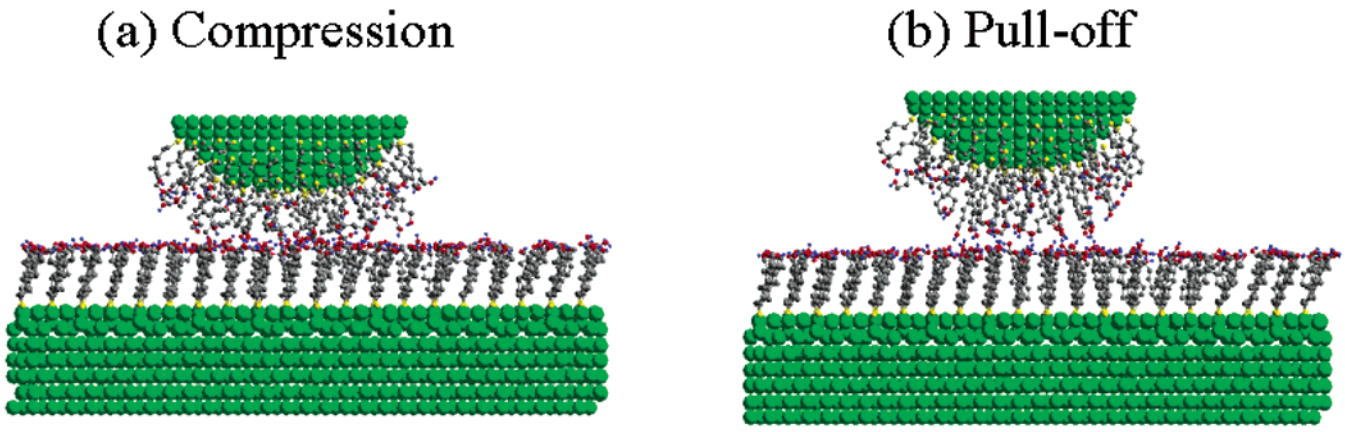

Figure 5. Molecular configurations for the OH/OH pair at (a) compression and (b) pull-off stages.

agrees well with experimental results (30 ± 16 mJ/m^2)[2] and is also comparable to our earlier calculation result (37 mJ/m^2).[14] The motion of the tip versus support position z_M is presented in Figure 2b. Initially, the tip followed the support motion prior to the jump-to-contact stage. When the jump-to-contact (stage b in Figure 2a) occurred, the tip suddenly stuck to the sample surface, resulting in a tensile spring force. During the retraction process (c → d), the tip stuck to the sample surface until it approached the pull-off (stage d in Figure 2a). Before the two surfaces were peeled apart, the support was lifted up by about 3.4 nm, while the tip went up only by about 0.25 nm (see Figure 2b). This led to a large elongation of the spring (k_z), from which the normal force (adhesion) was built up. This detailed information regarding tip motion is not available from CFM experiments.

Molecular configurations corresponding to the compression and pull-off stages are shown in Figure 3. It can be seen from Figure 3a that, at the compression stage, where the mean contact pressure reaches about 0.2 GPa, the deformation of SAM chains makes the contact area larger than that at the pull-off stage, but no chain entanglement occurs. Molecular configurations in Figure 3 for the CH_3/CH_3 pair also show that, at the unstable pull-off point, a significant molecular gap developed, and the contact size shrank dramatically.

When CH_3-terminal groups were replaced by OH groups, it was interesting to observe that the adhesion force increased by about 4 times, as shown in Figure 4a, due to the formation of hydrogen bonding among OH groups. This phenomenon under dry conditions is quite different from that in water for the same contact pairs, where solvent exclusion dominates adhesion.[5] It can be seen from Figure 4b that stronger binding between OH/OH contact pairs further elongated the spring k_z to about 10.0 nm at the pull-off stage. Comparison with the CH_3/CH_3 pair is

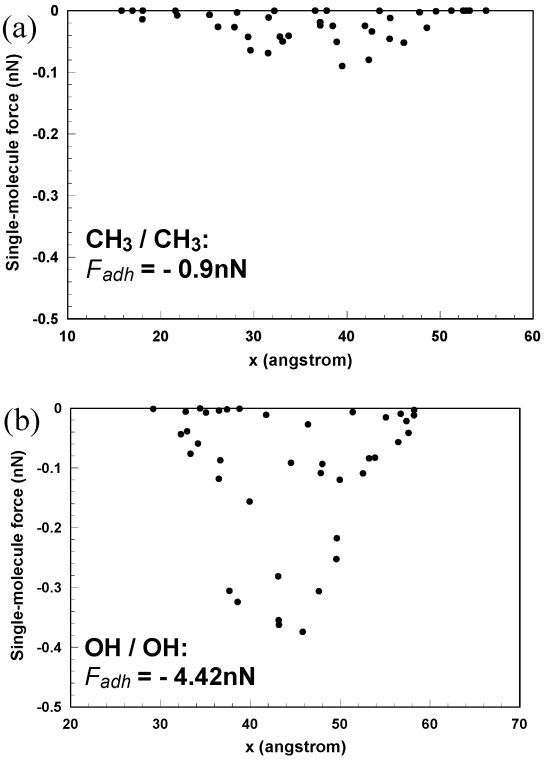

Figure 6. Single-molecule force distributions over SAM chains on the CFM tip at the pull-off stage for (a) CH_3/CH_3 and (b) OH/OH contact pairs.

also presented in the figure. Molecular configurations corresponding to compression (stage c) and pull-off (stage d) are shown in Figure 5. From eq 8, the surface energy γ_{OH} of the hydroxyl surface was calculated to be as high as 157 mJ/m^2. This value is comparable to that of the carboxyl (COOH) surface (114 ± 27 mJ/m^2) measured in dry N_2.[2] Since the number of molecular bonds at the pull-off stage is 29 and the contact radius is estimated to be 1.5 nm (see below), the bond energy of the OH group is calculated to be 4.7 kcal/mol.[33] This value is also comparable to that of the COOH group measured in dry N_2(5 ± 2 kcal/mol).[2]

Single-Molecule Forces. The development of AFM[34] makes it possible to probe single-molecule mechanical properties.[4,6−9]

(31) Johnson, K. L.; Kendall, K.; Roberts, A. D. *Proc. R. Soc. London A* **1971**, *324*, 301. The validity of JKR theory was recently discussed.[32] In our hybrid simulations, we estimate the Tabor parameter[32] in the following way. The surface energy of the methyl group[2] is around 30 mJ/m^2; thus, the work of adhesion w is equal to 60 mJ/m^2. The SAM chain length is comparable to the radius of a passivated Au tip, so the overall elasticity is controlled by the SAM film, which has an effective elastic modulus E^* around 1.0 GPa.[4] Suppose that the tip radius is $R = 3$ nm and the molecular gap at the pull-off stage is $z_0 = 1$ Å; then the Tabor parameter is calculated to be $\mu = (Rw^2/E^{*2}z_0^3)^{1/3} = 2.2$, which is in the JKR range ($\mu > 1.0$). In CFM experiments, since the apparatus has a finite stiffness, the unstable pull-off point will shift slightly relative to the JKR unstable point (soft machine with load control) (see: Greenwood, J. A. *Proc. R. Soc. London A* **1997**, *453*, 1277). Therefore, eq 8 still holds.

(32) Johnson, K. L.; Greenwood, J. A. *J. Colloid Interface Sci.* **1997**, *192*, 326.

(33) The hydrogen-bonding energy for the OH/OH pair was calculated as the total surface energy minus the van der Waals contribution that was assumed to be the surface energy for the CH_3/CH_3 pair.

(34) Binnig, G.; Quate, C. F.; Gerber, Ch. *Phys. Rev. Lett.* **1986**, *56*, 930.

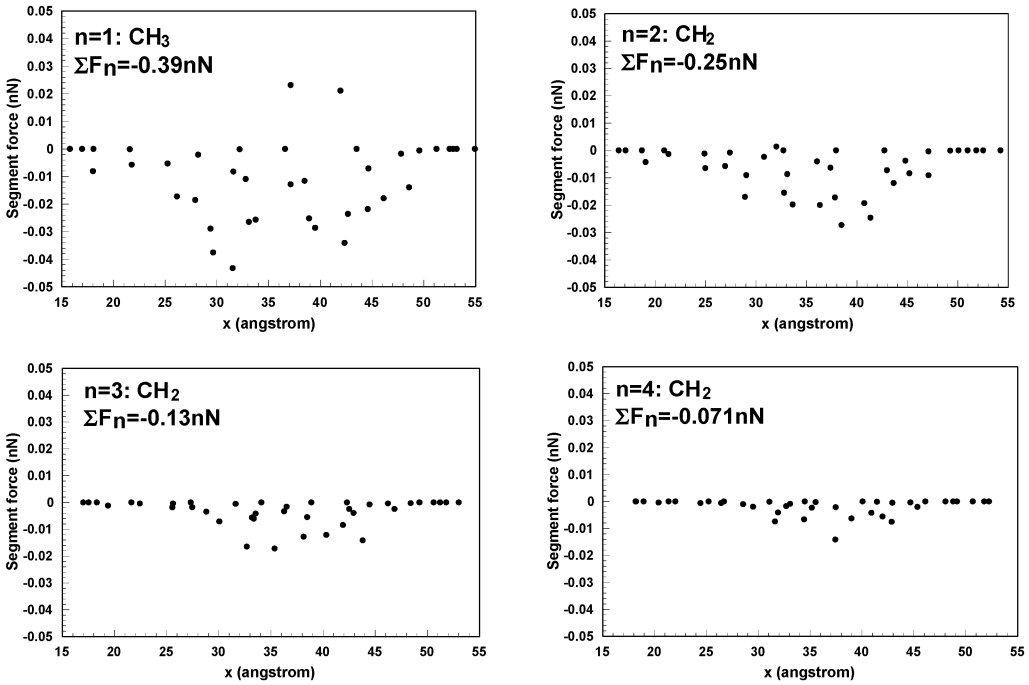

Figure 7. Segment force distributions over the individual segments of SAM chains on the CFM tip at the pull-off stage for the CH_3/CH_3 contact pair.

Force quanta measurement[8,9] and Poisson statistics method[6,7] are usually used to evaluate the mechanical strength of individual chemical bonds. However, detailed information about the load distribution among individual molecular chains or even segment-load distribution within the chains is still lacking. Molecular simulation provides a convenient way to determine these detailed molecular properties at the interface. Figure 6a,b shows single-molecule force distributions over 40 SAM chains on the CFM tip at the pull-off stage for CH_3/CH_3 and OH/OH pairs, respectively.[35,36] Contrary to one important assumption in the Poisson statistic method,[6] discrete bond forces do *not* distribute evenly. Instead, they vary across the tip and exhibit a maximum at the contact center. As shown in Figure 6a, for the CH_3/CH_3 pair, the number of bonds having forces greater than 10 pN is 22, and the mean single-molecule force over all SAM chains is 40 pN. The maximum bond force, however, can be as high as 80 pN. As shown in Figure 6b, for the OH/OH pair, the number of bonds having forces greater than 10 pN is 29, and the mean single-molecule force is 152 pN. The maximum bond force, however, can be as high as 380 pN. It can be estimated from Figure 6 that the contact radius (defined as the distance from the contact center to the edge where the force falls to zero) is approximately 1.5 nm for both contact pairs.

We now consider how these forces are distributed over the individual segments of SAM chains on the CFM tip. For the CH_3/CH_3 pair, Figure 7 shows the segment force distributions of the upper four UA atoms (one CH_3 and three CH_2). It can be seen that the first four segments have 94% load-bearing capacity. Moreover, even at the pull-off stage, some CH_3 groups still have a positive contact load. As shown in Figure 8, segment force distributions for the OH/OH pair are much more complicated due to the formation of hydrogen bonding. A large portion of the total load (about 86%) was borne by the first two segments, H and O, and many segment forces show positive contact loads.

Friction. Both friction and adhesion forces originate from molecular interactions at the interface and correlate with each other.[1,3,4] Early theory[37] states that the friction force F increases linearly with the contact load F_n:

$$F = \alpha F_n + F_0 \tag{9}$$

The constants α and F_0 depend on the chemical composition of the interface[3] and the actual contact area A_{real}. Equation 9 divided by A_{real} yields a relationship between the mean shear stress τ and the mean contact pressure p:

$$\tau = \alpha p + \tau_0 \tag{10a}$$

or

$$\mu_k = \tau/p = \alpha + \tau_0/p \tag{10b}$$

If p is much greater than τ_0, then μ_k will be constant, and Amonton's law of kinetic friction will apply.[38,39] For single asperity contact in CFM experiments and in our CFM simulations, SAM chains are too soft to support large loads, and τ_0 is large as compared to p. Therefore, Amonton's law is not valid. However, eqs 9 and 10 still hold. Instead of measuring μ_k, α is usually measured and referred to as the friction coefficient.[3,4]

Figure 9 shows typical friction loops for CH_3/CH_3 and OH/OH pairs under a contact load of 0.2 nN. The friction force for the OH/OH pair is much larger than that of the CH_3/CH_3 pair due to the breaking/formation of hydrogen bonds. Mean friction

(35) Mean single-molecule force is defined in our simulations as all van der Waals interactions exerted on CH_3-terminated SAM chains on the CFM tip by substrate SAM chains divided by the number of chains involved in interactions. In CFM experiments, total interactions are measured and divided by the estimated number of chains at the interface.

(36) Similarly, the calculated mean single-molecule force for the OH/OH pair is the *total* force, i.e., the sum of van der Waals and hydrogen-bonding forces, exerted on SAMs on the CFM tip by substrate SAM chains.

(37) Briscoe, B. J.; Evans, D. C. B. *Proc. R. Soc. London A* **1982**, *380*, 389.
(38) Bowden, F. P.; Tabor, D. *The Friction and Lubrication of Solids*; Oxford University Press: Oxford, 1958.
(39) He, G.; Muser, M. H.; Robbins, M. O. *Science* **1999**, *284*, 1650.

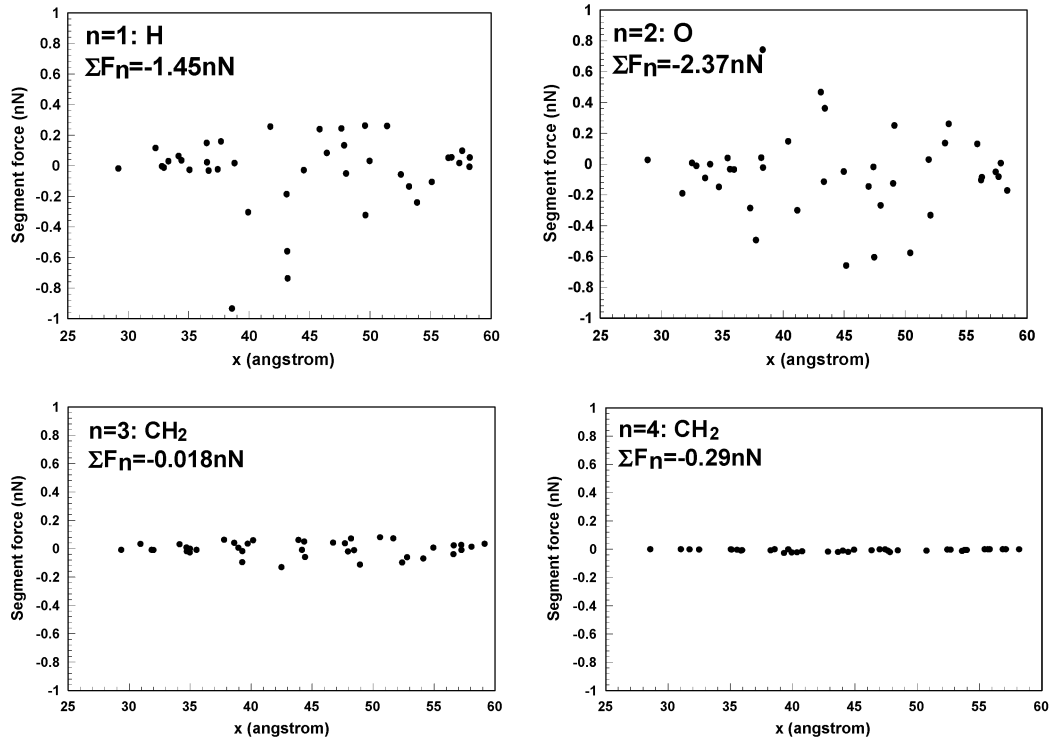

Figure 8. Segment force distributions over the individual segments of SAM chains on the CFM tip at the pull-off stage for the OH/OH contact pair.

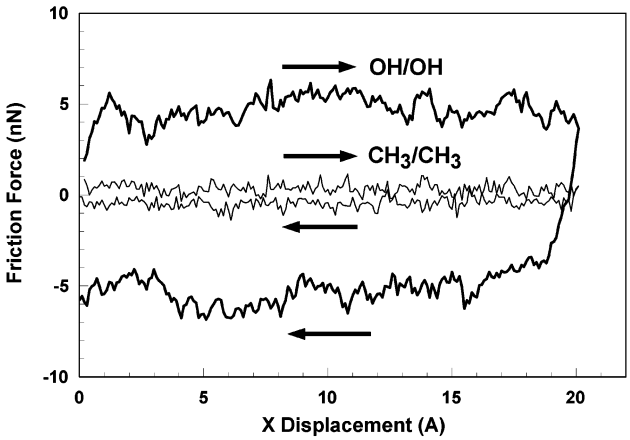

Figure 9. Typical friction loops for the CH_3/CH_3 and OH/OH pairs under a contact load of 0.2 nN.

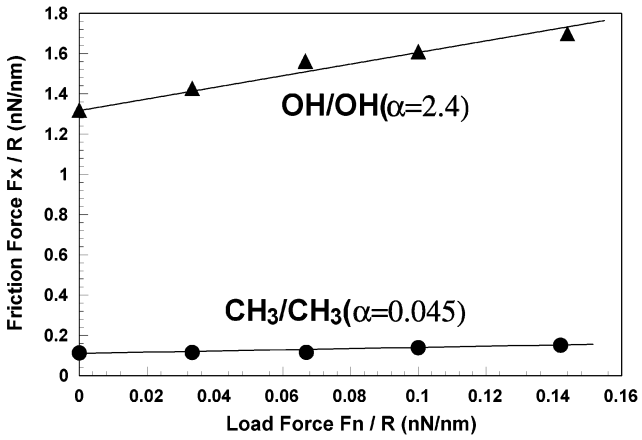

Figure 10. Friction force versus contact load for CH_3/CH_3 and OH/OH contact pairs.

force vs contact load curves are shown in Figure 10. These forces are reduced by the tip radius R and are comparable to those obtained from CFM experiments.[1] As shown in Figure 10, the maximum contact pressure in our simulations is 0.06 GPa. However, the corresponding shear stresses reach 0.68 and 0.06 GPa for OH/OH and CH_3/CH_3 pairs, respectively. Friction coefficients α for CH_3/CH_3 and OH/OH pairs are 0.045 and 2.4, respectively. These values are comparable to those of methyl-terminated surfaces ($\alpha = 0.07$) and the hydrophilic COOH/COOH contact pair ($\alpha = 1.0$) measured in argon at room temperature.[3] Specially, strong adhesion due to hydrogen bonding leads to an increase in the initial constant F_0 and the slope (friction coefficient α) for the cases studied here.

Conclusions

We have demonstrated that the temporally hybrid method recently developed by us is well suited to simulating adhesion and friction processes in CFM experiments on the experimental time scale. Various properties for hydrophobic CH_3/CH_3 and hydrophilic OH/OH contact pairs were studied, including force−distance curves, actual tip position vs support position, single-molecule force distributions, friction loops, friction force vs contact load force curves, and molecular structures. The formation of hydrogen bonds for the OH/OH contact pair makes the adhesion force and surface energy of OH-terminated surfaces 4 times larger than those for the CH_3/CH_3 contact pair. For both CH_3/CH_3 and OH/OH contact pairs, CFM tip position vs cantilever support position curves show that, during the retraction of a CFM tip from a surface, the CFM tip is away from the sample surface slightly while the spring undergoes dramatic elongation in the normal direction before rupture occurs. Even at the compression stage, under a contact pressure of 0.2 GPa, no chain entanglement occurs. Single-molecule forces at the contact area *do not* distribute evenly. This is in contrast to one

important assumption, under which the Poisson statistic method is often used to evaluate the mechanical strength of individual chemical bond. Force distributions over the individual segments of SAM chains on the CFM tip are much more complicated. Even at the pull-off point, some of them exhibit positive contact load. Finally, surface energies and friction coefficients calculated for hydrophobic and hydrophilic interfaces compare well with those from CFM experiments.

Acknowledgment. This work is supported by the Surface Engineering and Material Design (SEM) Program of the National Science Foundation, Grant No. CMS-9988745.

JA026274Z